Summer Internship Report - Goodwin Group

Zoe Faure Beaulieu

29^{th}June 2020 - 4^{th} September 2020

Contents

1 Aims

The aim of the project was to determine whether vacancy ordering could lead to the emergence of bulk ferrimagnetism in a key family of guanidinium transition-metal formate perovskites. The project was split into two parts: one computational and one experimental.

2 Monte Carlo Simulations

A series of Monte Carlo simulations were carried out to confirm the threshold composition for vacancy order. A given fraction ($\frac{x}{3}$, x = 0.05, 0.10, 0.20,..., 1.0) of vacancies was randomly allocated on the lattice and the remaining sites treated as occupied. The simulation was then run by simulated annealing until the ground state was reached. For this, only nearest-neighbour interactions were considered and the energy of the systems before and after were calculated according to equation 1.

$$H = -J \sum_{<ij>} s_i s_j \tag{1}$$

A vacancy order paramater was then calculated according to

$$F\left(\mathbf{k}\right) = \frac{\left| \frac{1}{N} \sum_i^N \left(s_i - \langle s \rangle\right) \exp\left[2\pi \mathrm{i} \mathbf{k} \cdot \mathbf{r}_i\right] \right|^2}{4(1 - n_a)^2} \tag{2}$$

The sum runs over all the positions i of the matrix with N being the number of elements, s_i the state of the element i and r_i the position vector of element i. k is known as the reciprocal space vector, it corresponds to the positions at which the new reflections should be found - in this case k is $\left(\frac{1}{2}, \frac{1}{2}\right)$ and $\left(\frac{1}{2}, -\frac{1}{2}\right)$. The following plots were obtained, clearly showing an ordering of vacancies around the percolation threshold for the FCC lattice (x=0.6)

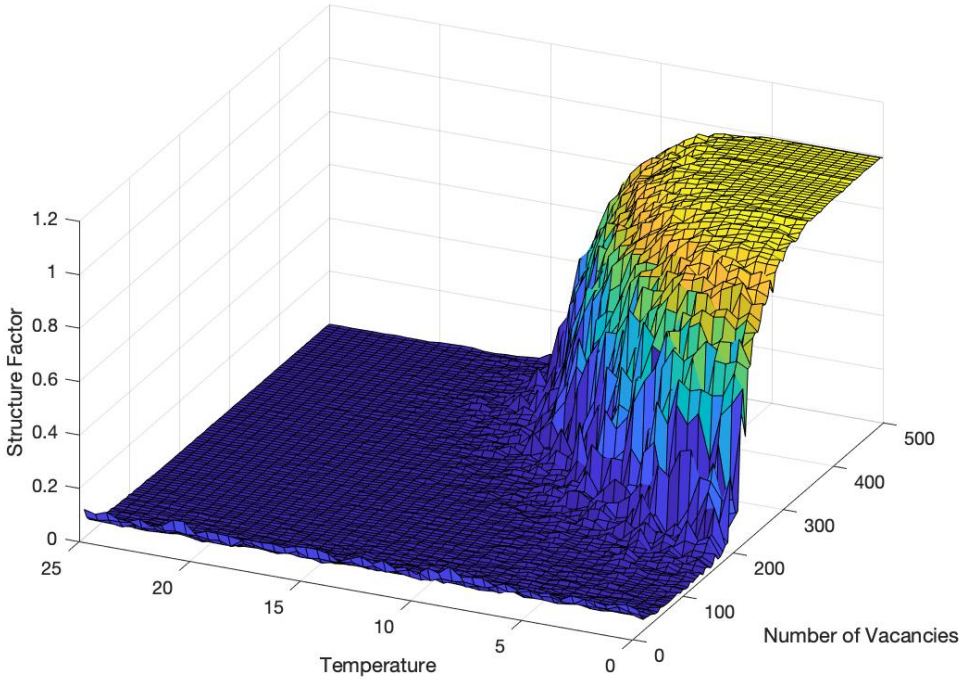

Figure 1: Structure Factor vs Temperature and Vacancy Number for a 10x10x10 lattice

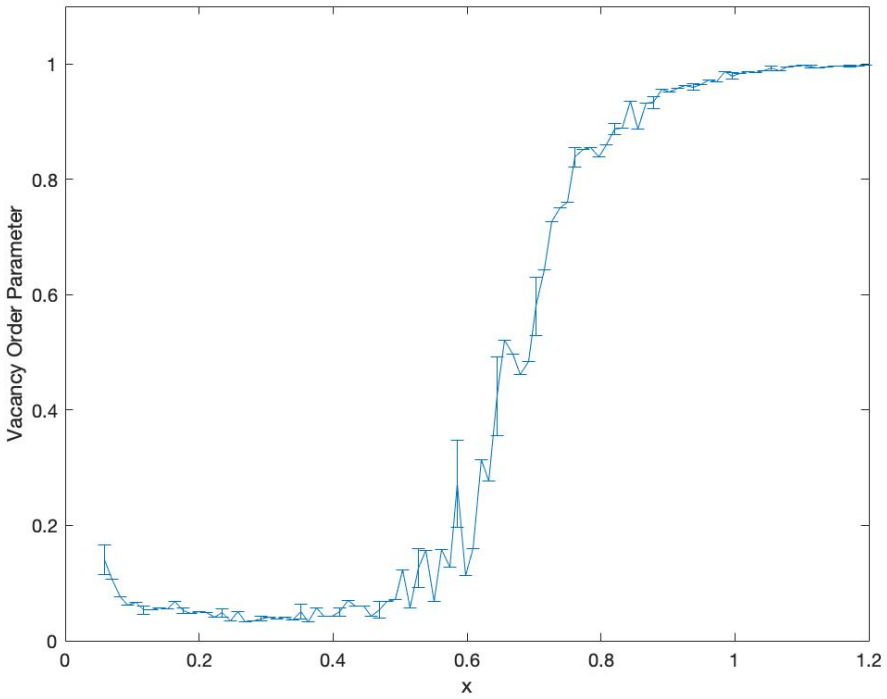

Figure 2: Vacancy order parameter vs x for an 8x8x8 lattice

The final step was to simulate magnetic susceptibility. To do this, I utilised code by Joe Paddison which models the magnetic spins according to the Heisenberg Model. The aim being to observe a jump in suscpetibility around the percolation threshold and a large increase in susceptibility as the temperature is lowered according to figure 3 below:

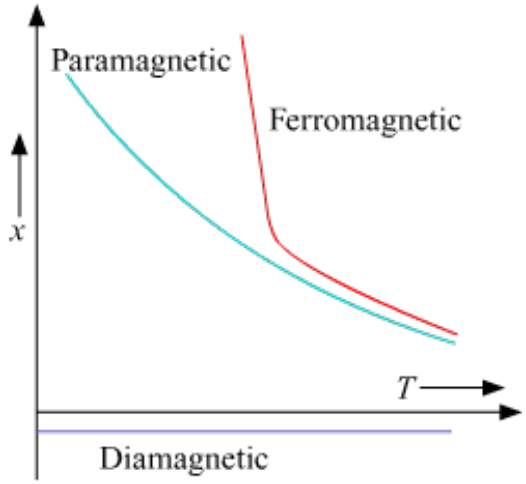

Figure 3: Magnetic susceptibility vs T for various magnetic behaviours

The results can be seen in figures 4 and 5. The desired behaviour is clearly observed and indicates that vacancy ordering has led to a the emergence of bulk ferrimagnetism.

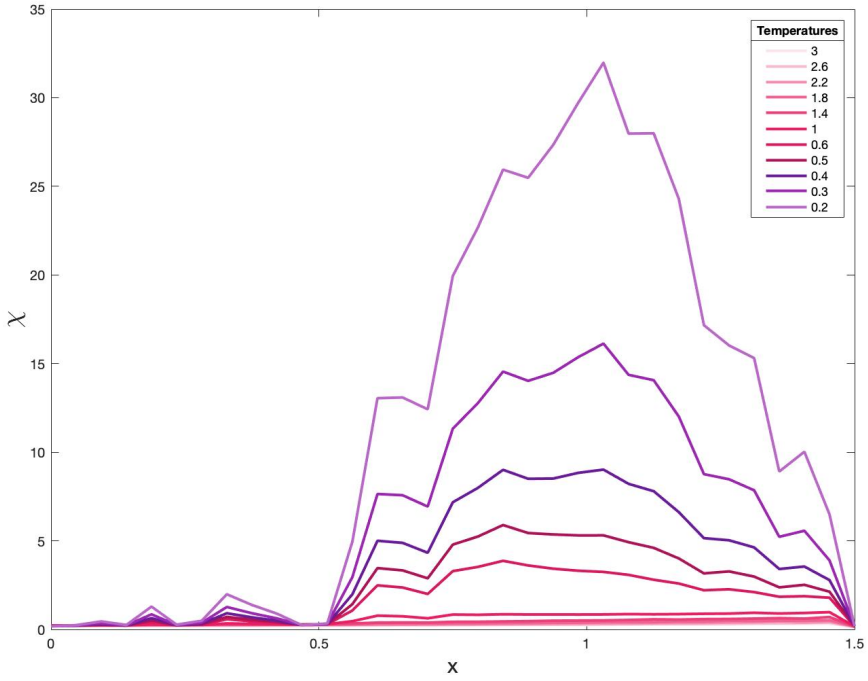

Figure 4: Magnetic susceptibility vs x for various temperatures

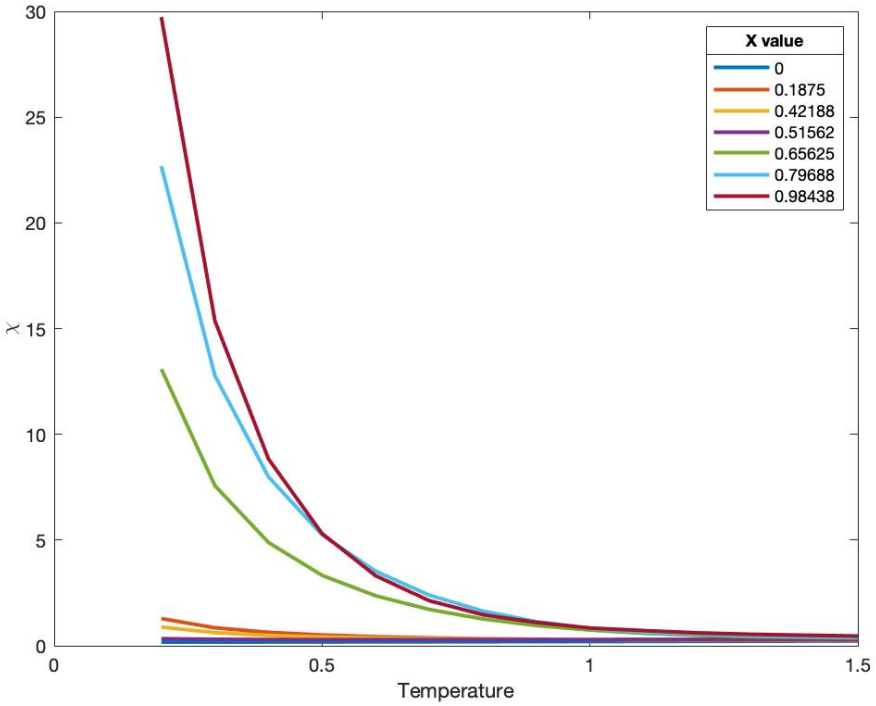

Figure 5: Magnetic susceptibility vs T for various compositions

3 Experimental Methods

Once it had been establised that ferromagnetic behaviour should be observed beyond the percolation threshold, the next step was to confirm these results experimentally.

3.1 Synthesis

Polycrystalline samples of general formula $[C(NH_2)_3]Mn^{2+}_{1-x}(Fe^{3+}_{2x/3},\square_{x/3})(HCOO)_3$ where x = 0,0.05,0.1,0.2,...,1.0, were synthesised. Three methanolic solutions were made, the first contained 4.05g of $[C(NH_2)_3]_2CO_3$ and 2.63mL HCOOH dissolved in 71.9mL of methanol. The other two were: a 0.1M solution of $FeCl_3$ and a 0.1M solution of $Mn(ClO_4)_2$. The three solutions were mixed in the relevant ratios: 5(1-x)mL of 0.1M $Mn(ClO_4)_2$, 5xmL of 0.1M $FeCl_3$ and 5mL of the acidified guanidium solution. They were then sealed and left to stir at room temprature overnight. Once completed, the solutions were filtered *in vacuo*, the crystals washed with methanol and dried overnight in the vacuum oven. The colour of the samples ranged from white to pale ochre as x increased. A total of 12 samples were made

3.2 Powder X-Ray Diffraction

To confirm that the correct samples were synthesised, the X-Ray diffraction patterns of each one was obtained. Figure 6 shows the Pawley fits of the X-ray patterns.
The emergence of additional peaks beyond x = 0.6 confirms the change in space group from orthorombic *Pnna* to monoclinic $P\frac{2}{n}11$.

It was decided that the higher Fe samples would be redone (according the synthesis outlined in section 3.1) as the quality of the powder patterns reduced significantly as x increased - see figure 7. It was suggested that this was due to the $FeCl_3$ being old and therefore accumulating significant amounts of water.
I was able to synthesise and filter the new high-content Fe samples but not able to obtain X-ray patterns as my internship can to an end.

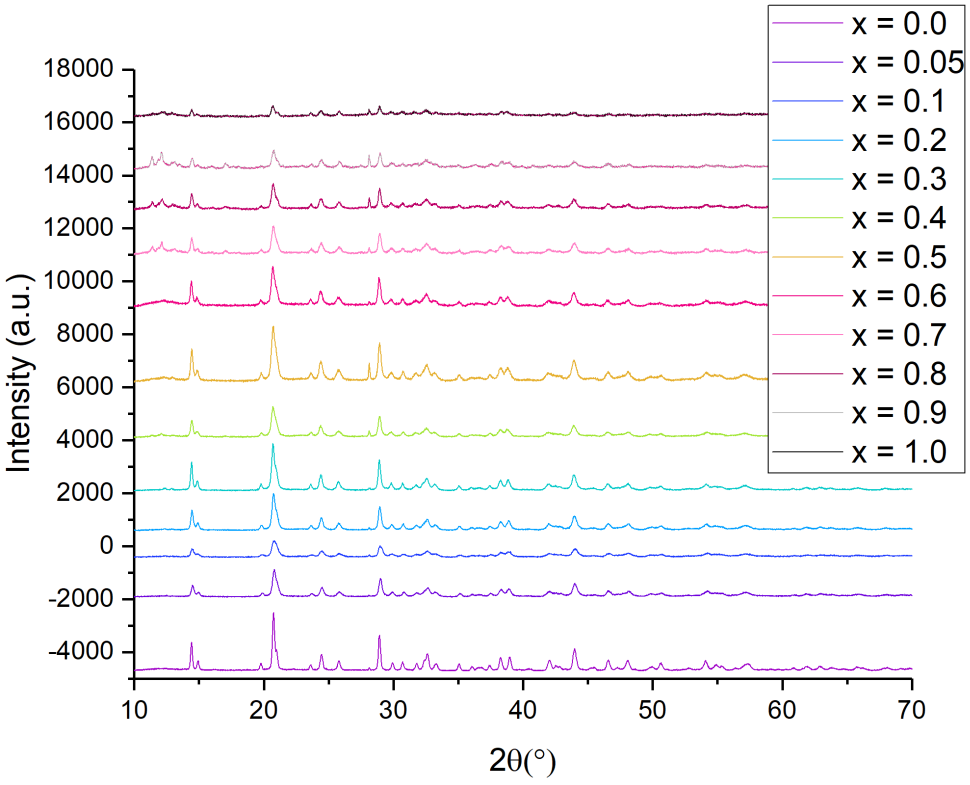

Figure 6: X-ray Diffraction patterns for x=0 to x=1

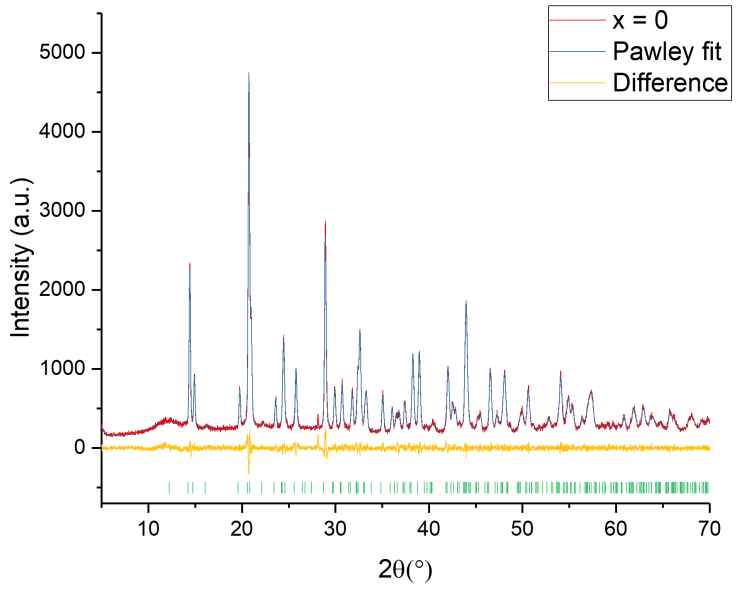

(a) x = 0

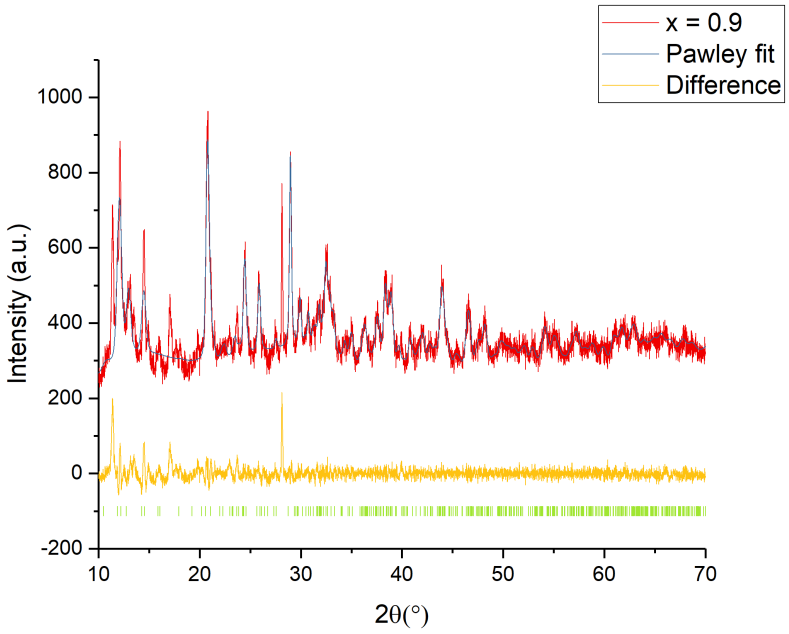

(b) x = 0.9

Figure 7: Pawley fit of the X-ray powder diffraction pattern of the x = 0 sample and x = 0.9 sample. The calculated pattern is shown in blue, observed data in red, difference curve in orange, allowed hkl positions in green.

3.3 SQUID Measurements

Due to time constraints I was not able to carry out SQUID measurements on the majority of my samples. These will be carried out at a later stage by the Goodwin Group to confirm the presence of ferrimagnetism in the high Fe content samples.
SQUID measurements were carried out on the x = 0 samples and the following plot obtained.

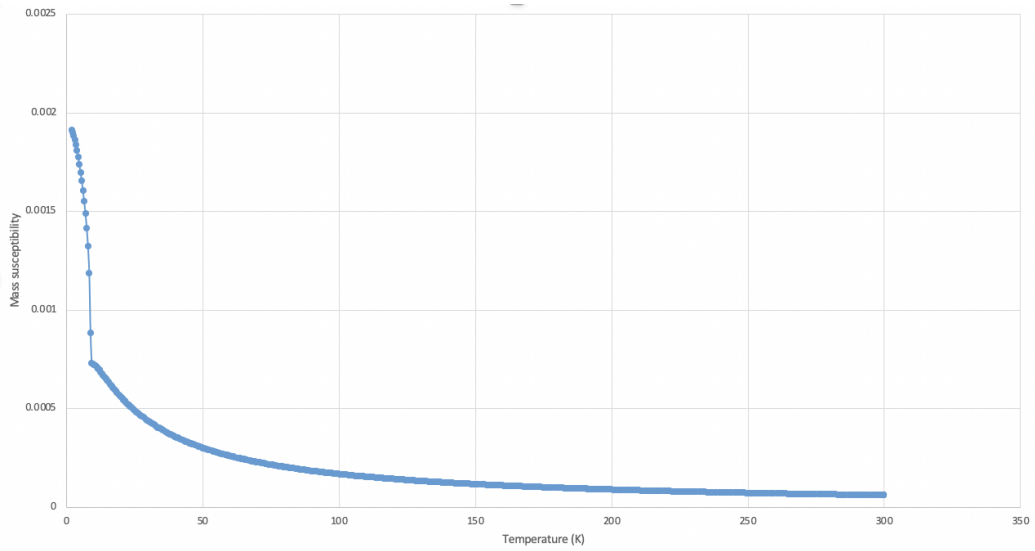

Figure 8: Mass Susceptibility vs Temperature for x = 0 sample